Elastic Modulus of Amorphous Polymer Thin Films: Relationship to the Glass Transition Temperature

Jessica M. Torres,[†] Christopher M. Stafford,[‡] and Bryan D. Vogt[†,*]

[†]Department of Chemical Engineering, Arizona State University, Tempe, Arizona 85284, and [‡]Polymers Division, National Institute of Standards and Technology, Gaithersburg, Maryland 20899

O ne of the fundamental principles in understanding the viscoelastic properties of polymers is time−temperature superposition, which enables the collapse of temperature and rate dependencies of the complex modulus to a single master curve.[1,2] This correlation enables prediction of the mechanical properties of polymers at long time scales. Williams, Landel, and Ferry (WLF) illustrated the use of a single empirical shift factor and a reference temperature to correlate the rheological data for several macromolecules.[1] The glass transition temperature (T_g) is commonly employed as the reference condition due to the viscoelastic behavior of the polymer being extremely sensitive to temperature near T_g.[3] This relationship between T_g and mechanical properties in the bulk has been proposed to also apply to polymers at the nanoscale.[4,5] This predictive ability at the nanoscale is essential since the long-term mechanical stability of polymer nanostructures is critical for numerous developed and emerging applications including photonics,[6] microelectronics,[7] nonlinear optics, and biosensors.[8] For example, the microelectronics industry relies on the mechanical robustness of polymeric photoresists to enable patterning of submicrometer features; decreases in the mechanical properties at small length scales would be detrimental to patterning for next generation lithography.[9] In nanoimprint lithography,[10] for example, the flow resistance of polymer melts in confined geometries has recently been reported to decrease when the slit width is comparable to the molecular dimensions of the polymer,[11] which has implications in the processing of imprinted structures. Moreover, the molded structure has tremendous residual stress,[12] thus understanding the elastic modulus in confined

ABSTRACT Understanding the mechanical properties of polymers at the nanoscale is critical in numerous emerging applications. While it has been widely shown that the glass transition temperature (T_g) in thin polymer films generally decreases due to confinement effects in the absence of strong favorable interactions between the polymer and substrate, there is little known about the modulus of sub-100 nm polymer films and features. Thus, one might use this depressed T_g as a surrogate to estimate how the modulus of nanoconfined polymeric materials deviates from the bulk, based on constructs such as Williams−Landel−Ferry (WLF) time−temperature superposition principles. However, such relationships have not been thoroughly examined at the nanoscale where surface and interface effects can dramatically impact the physical properties of a material. Here, we measure the elastic modulus of a series of poly(methacrylate) films with widely varying bulk T_g's as a function of thickness at ambient temperature, exploiting a wrinkling instability of a thin, stiff film on an thick, elastic substrate. A decrease in the modulus is found for all polymers in ultrathin films (<30 nm) with the onset of confinement effects shifting to larger film thicknesses as the quench depth ($T_{g,bulk} − T$) decreases. We show that the decrease in modulus of ultrathin films is not correlated with the observed T_g decrease in films of the same thickness.

KEYWORDS: thin films · elastic modulus · wrinkling · glass transition · polymers · confinement

geometries is also critical to the stability of structures formed *via* nanoimprint lithography.

The simplest example of a polymer confined to nanometer length scale is a thin film where the thickness of the film is less than 100 nm. The physical behavior of polymer films can provide insight into the behavior of more complex or even nanostructured polymer materials, such as nanocomposites.[13,14] Research to date has primarily focused on elucidating the confinement effect of T_g in thin films due to the interdependency between T_g and other physical properties for bulk polymers.[15−19] Attempts to understand confinement effects[20] have progressed in two distinct directions: first, the importance of interfaces and interfacial interactions[15,21] and, second, a fundamental examination of the controlling length scales such as molecular weight[16,22,23] and cooperative rearrangement length, ξ(CRR), of the polymer

*Address correspondence to bryan.vogt@asu.edu.

segments.[22] Despite its technological importance, the corresponding modulus of confined thin polymer films has yet to be fully characterized to the extent that T_g effects have been. Interestingly, simulations by Bohme and de Pablo suggest the existence of significant stress relaxation occurring at the air−polymer interface even at temperatures deep in the glass where a deviation in mechanical properties would not be expected.[24]

This prediction raises questions as to the relationship between the observed deviations in the T_g of polymer thin films and the modulus of such films. Unfortunately, direct experimental measures of the modulus of ultrathin, compliant materials have proven to be difficult since the presence of the stiff substrate tends to interfere with the measurement. For indentation-based measurements, substrate effects have been reported for films greater than 200 nm,[25] but the use of multiple layer modeling has enabled the elastic properties of thin (<100 nm) polymer films to be elucidated in select cases.[26] Van Vliet and co-workers have demonstrated that for glassy polystyrene (PS) and poly(methyl methacrylate) (PMMA) there is as much as a 200% increase in the surface stiffness as probed by nanoindentation within the first 200 nm.[27] They attribute this increase to the creation of a mechanically unique interfacial region confined between the indentation probe and the polymer surface.[27] Atomistic simulations of amorphous glasses such as silica and polymer nanostructures have also shown an increase in bending rigidity as the beam dimensions decrease.[28] However, by using an AFM to control the indentation depth, the top 5 to 7 nm of a PS film has been shown to have a significantly reduced elastic modulus.[29,30] This reduced surface modulus is consistent with the reduced surface T_g of PS[31] but is in conflict with the observed surface stiffening as determined by nanoindentation.[27] Moreover, Brillouin light scattering (BLS) of free-standing PS films as well as nanoimprinted polymer structures shows no apparent change in the PS mechanical stiffness for films as thin as 29 nm, despite the large depression in T_g (60 °C) from bulk.[32,33] Conversely, using controlled capillary forces, the modulus of poly(methyl methacrylate) (PMMA) nanostructures decreases when the width is less than approximately 100 nm,[34] while thin films of PMMA maintain a bulk-like modulus down to nearly 40 nm prior to a modulus reduction as determined by surface wrinkling measurements.[35] As different measurement strategies are developed and employed, there remains disagreement as to the impact of confinement on elastic modulus of soft materials: the modulus has been reported to increase,[27] decrease,[28,29,34] and not change,[32] similar to the initial polymer thin film T_g measurements.[36,37] In the case of thin film T_g, some of the initial conflicting results can now be rationalized by differences in the polymer−substrate interaction.[38] Similarly, the nature of the probe interaction for indentation measurements could impact the observed mechanical

TABLE 1. Physical Characteristics of Polymethacrylates Used in This Study

polymer	M_w (kg/mol)	T_g (°C)
poly(methyl methacrylate)	91	105
poly(ethyl methacrylate)	250	65
poly(n-propyl methacrylate)	70	36
poly(benzyl methacrylate)	70	54
poly(isobutyl methacrylate)	200	47

properties. Thus, noncontact mechanics measurements that do not disturb the free surface appear to be potentially advantageous for elucidating the modulus of polymer films and nanostructures.

From previous studies utilizing wrinkling of films, the reduced modulus ($\bar{E}_f/\bar{E}_{bulk}$, ratio of thin film to bulk elastic modulus) for PS and PMMA thin films was found to exhibit statistically identical behavior with deviations from the bulk modulus at approximately 40 nm at ambient temperature.[35] Simulations have suggested that deviations in the modulus of films when the polymer is deep in the glass should occur near 40 nm,[24] which is in agreement with these experimental results for PS and PMMA thin films. However, 40 nm is also close to the length scale where changes in the thin film T_g are typically observed.[39,40] To facilitate a clearer understanding of the relationship between depressed T_g and elastic modulus of ultrathin polymer films, experiments need to be conducted closer to the glass transition temperature rather than deep in the glassy state. It is in this region that the mechanical properties of bulk polymeric materials exhibit increased cooperativity and molecular motions that lead to a dramatic decrease in modulus. With this knowledge, we will be able to establish whether fundamental scaling concepts such as the WLF equation, considered basic tenets of polymer science, indeed hold true at the nanoscale. Demonstrating whether these concepts are applicable at the nanoscale, as well as when and how they break down, will be critical to nanomanufacturing and understanding the reliability of nanoscale polymeric materials.

In this paper, a series of methacrylate polymers are examined to determine how the quench depth ($T_{g,bulk}$ − T) impacts the "critical thickness" where the moduli of thin films deviate from the bulk. This quench depth into the glassy state provides a measure of the proximity to the liquid state for the bulk of each polymer examined. The use of methacrylate polymers allows for the quench depth to be readily varied without requiring *in situ* heating or cooling during the experiments, as T_g is significantly impacted by alkyl chain length, as shown in Table 1.[41] Moreover, the chemistry difference is less for these methacrylate polymers than between PMMA and PS examined previously.[35] Thus, we hypothesize that the chemistry effects from changes in the alkyl chain length from methyl to *n*-propyl on the thin
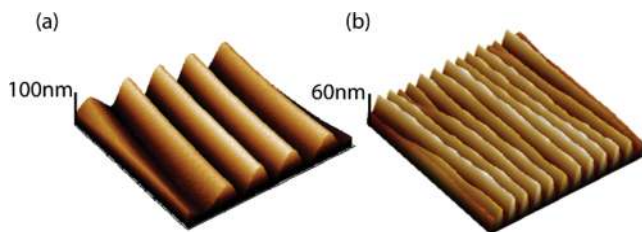
Figure 1. AFM image of wrinkled P*n*PMA films having a thickness of (a) 40 nm and (b) 10 nm supported on PDMS. Scan size is 7.5 μm × 7.5 μm. The height scale for the images is (a) 100 nm and (b) 60 nm as noted in the images.

film modulus behavior will be minor in comparison to the large changes in quench depth.[24,42]

RESULTS AND DISCUSSION

To elucidate the modulus of thin polymer films, a wrinkling instability is utilized that arises upon compression of a stiff film bonded to a compliant substrate, as described in detail elsewhere.[43−47] A more detailed description is also included in Supporting Information. The film modulus ($\bar{E}_f$) is related to the substrate modulus ($\bar{E}_s$), the film thickness (h_f), and the wrinkling wavelength (λ) by

$$\bar{E}_f = 3\bar{E}_s\left(\frac{\lambda}{2\pi h_f}\right)^3 \tag{1}$$

Accurate metrologies for determining both the film thickness and the modulus of the substrate are well-established, thereby allowing for the determination of the film modulus by measuring λ.[48] Figure 1 illustrates the sinusoidal structure resulting from the wrinkling of poly(*n*-propyl methacrylate) (P*n*PMA) films of different thickness on poly(dimethylsiloxane) (PDMS) substrates. PDMS is a cross-linked elastomer with an elastic modulus (≈1 MPa) that is orders of magnitude less than the bulk modulus of any of the methacrylate polymers examined here. The bare PDMS surface is smooth and featureless[35] with a typical rms roughness less than 1 nm (see Supporting Information). The AFM micrographs in Figure 1 illustrate the decrease in wavelength for thinner films as expected from eq 1. Application of eq 1 to calculate the modulus of the film yields a modulus for the 10 nm film (0.04 GPa) that is dramatically less than that for the 40 nm film (0.58 GPa). Qualitatively, this result is consistent with previous reports of a reduced modulus in polymer thin films.[35]

Further examination of this system indicates that the modulus of P*n*PMA films appears to deviate from the bulk value at a thickness of nearly 80 nm, as shown in Figure 2. This length scale for observed changes in the modulus is consistent with simulations when approaching $T_{g,bulk}$.[24] This begs the question as to whether the T_g of P*n*PMA films is also impacted on this size scale? It is known that the glass transition temperature of supported thin polymer films is strongly dependent upon the interactions with the substrate. Thus to compare the changes in thin film modulus and T_g, identical substrate

interactions should be considered. Fortuitously, P*n*PMA films thicker than approximately 50 nm are stable on a PDMS surface in the rubbery state (no dewetting), thus enabling the T_g of the films to be measured from the discontinuity in the coefficient of thermal expansion between the glassy and rubbery state. Interestingly, the T_g of P*n*PMA films on PDMS does not statistically vary as the thickness is decreased down to nearly 50 nm, as shown in Figure 2. This result suggests that typical deviations in the apparent T_g of thin films, as measured by X-ray reflectivity,[49,50] ellipsometry,[17,39] and Brillouin light scattering[40,51,52] do not necessarily correlate with the size scales where changes in the mechanical properties of polymers occur. Novel bubble rheology experiments from McKenna and co-workers showed changes in the rheological properties of thin polymer films where no change in the T_g was observed.[53] Additionally, Forrest *et al.* demonstrated that mechanical properties of free-standing PS films did not correlate with changes in thin film T_g as determined by BLS.[32] It should be noted that nonmechanical properties, such as physical aging,[54] have also shown quantitative differences in thickness dependencies in comparison to thin film T_g. The modulus of the P*n*PMA thin films also shows a thickness dependence that is not consistent with T_g variation. Simulations suggest that the free surface mobility/relaxations are responsible for the decrease in the modulus of polymer thin films.[24,42] The lack of correlation between the length scale for thickness-dependent modulus and T_g raises questions as to the relevant parameters that control the mechanical stability of polymeric nanostructures.

According to simulations, the quench depth into the bulk glassy state is an important factor in determining the thickness at which deviations in elastic modu-
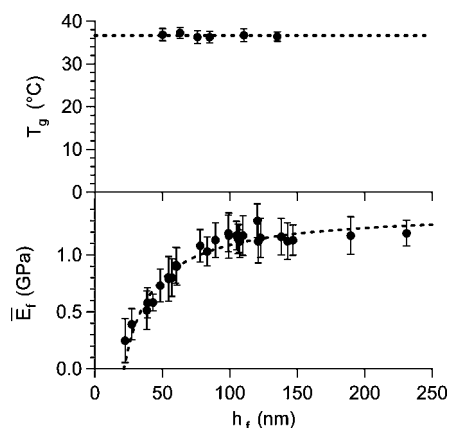
Figure 2. Comparison of the T_g and moduli of P*n*PMA thin films on PDMS. The dashed line in the upper panel is a guide to show that T_g is independent of film thickness over the range examined. The dashed line in the lower panel is a fit of the moduli data to a bilayer model (see text for details). The error bars represent one standard deviation of the data, which is taken as the experimental uncertainty of the measurement.
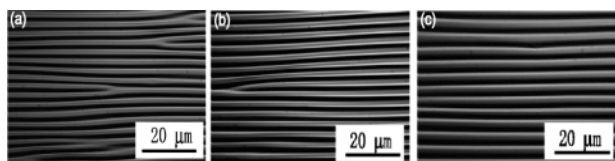
Figure 3. Optical micrographs of wrinkled ≈100 nm thick films of (a) PnPMA, (b) PEMA, and (c) PMMA. Note that the wavelength of the wrinkles decreases from PMMA to PEMA to PnPMA corresponding to a decreasing modulus in this series of polymers.
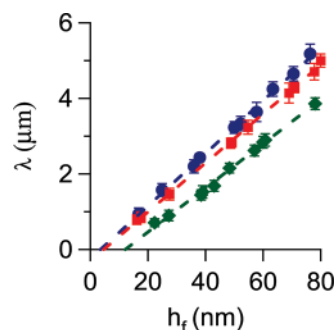

Figure 4. Wrinkling wavelength as a function of film thickness for PMMA (●), PEMA (■), and PnPMA (♦). The extrapolated wavelength-thickness correlation deviates from the origin, consistent with thickness-dependent moduli. The dashed lines are linear fits to the data, and the error bars represent one standard deviation of the data, which is taken as experimental uncertainty of the measurement.

lus occur in thin films.[42] These simulations suggest a soft layer near the free surface, and the thickness of this layer approaches that of the film as T_g is approached.[42] To physically explain this behavior, fast segmental motions near the free surface[55−57] are suggested to initiate cooperative motion of many segments and enhanced polymer mobility[58] leading to a decrease in modulus. Although temperature-dependent measurements of the modulus would be preferred, the *in situ* heating of a polymer−PDMS bilayer through all processing steps and characterization is impractical. Instead, a constant temperature ($T = 22 \pm 2$ °C) is utilized in these studies. The influence of quench depth is thus probed by variation in polymer chemistry to examine materials with widely varying T_g's; the series of poly(n-alkyl methacrylate)s represents an ideal series where T_g can be varied from well above ambient to below ambient, simply by increasing the length of the alkyl chain from methyl to n-butyl. Figure 3 shows optical micrographs for approximately 100 nm thick films of PMMA, poly(ethyl methacrylate) (PEMA), and PnPMA that are wrinkled on a PDMS substrate. By changing the polymer chemistry, quench depths of approximately 83, 43, and 14 °C, respectively, can be realized. One salient feature of this model system is that the wavelength of the wrinkles also decreases as the alkyl chain length increases; this corresponds to a lower modulus in the longer alkyl polymers, as expected.

Previous work examining the modulus of thin PS films demonstrated that the wrinkle wavelength as a function of film thickness can provide information about the length scale for a presumably low modulus surface layer.[35] Figure 4 illustrates the linear relationship between wrinkle wavelength, λ, and film thickness, h_f, for three poly(n-alkyl methacrylate)s on PDMS with nominally constant $\bar{E}_s$. The slope of the linear fits to the wavelength data decreases as the alkyl chain length is increased, which is consistent with a progressively smaller modulus for PMMA to PEMA to PnPMA. Additionally, the extrapolated wavelength does not extend through the origin. Instead, there appears to be a finite thickness (h_f*) where the film might be intrinsically stable (zero wavelength). This behavior has been previously reported for PS thin films and is attributed to free surface effects.[35] For the case of PS, h_f* was only 2 nm, consistent with a proposed liquid-like surface layer from other measurements on PS thin films.[44] A

liquid-like (low modulus) surface layer of thickness h_f* could not sustain wrinkling, so any film that is thinner than h_f* would show in essence a wrinkling wavelength of zero. In the case of the poly(n-alkyl methacrylate)s examined here, much larger extrapolated thicknesses for null wavelength wrinkles are observed, up to nearly 25 nm for PnPMA. As the alkyl chain length increases (and subsequently the quench depth into the bulk glass is decreased), h_f* shifts to progressively larger values. This trend is consistent with simulations from de Pablo and coworkers, where they suggested that an increase in free surface mobility as bulk T_g is approached leads to a longer length scale over which the surface modulus is impacted.[42] Since the wavelength *versus* thickness should transverse the origin in the case of a constant film modulus according to eq 2, the moduli of these films appear to be thickness-dependent.

Figure 5 illustrates the calculated moduli, $\bar{E}_f$, as a function of film thickness for PMMA, PEMA, and PnPMA as determined using eq 1. The modulus for thick films (>100 nm) examined here was found to be independent of film thickness. By assuming a
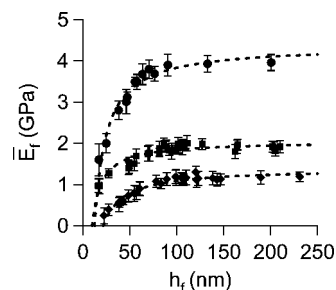

Figure 5. Elastic moduli of PMMA (●), PEMA (■), and PnPMA (♦) thin films as a function of film thickness. The PMMA and PEMA films show a decrease in apparent modulus at ≈60 nm, while the PnPMA film exhibits a decrease in apparent modulus at ≈85 nm. The lines are a fit to the bilayer model, and the error bars represent one standard deviation of the data, which is taken as the experimental uncertainty of the measurement.

Poisson's ratio of 0.33, the Young's moduli of these relatively thick polymer films were estimated to be 3.50, 1.70, and 1.06 GPa for PMMA, PEMA, and PnPMA, respectively. These moduli correspond well with the corresponding bulk moduli reported in the literature.[59−61] The modulus of PMMA decreases as the thickness of the film is decreased below $\approx$50 nm and reaches a value that is 48% of the bulk value (1.50 GPa) at $\approx$20 nm, in agreement with previous reports.[35] Increasing the alkyl chain from methyl to ethyl results in a deviation in modulus at slightly larger thicknesses ($\approx$57 nm). Similar to PMMA, PEMA also reaches 50% of its bulk value (0.87 GPa) at approximately 20 nm. Both polymers are well into the glassy regime with T_g's for bulk materials of 105 and 65 °C for PMMA and PEMA, respectively, in comparison to the measurement temperature used here, 22 ± 2 °C. The values of h_f* are comparable between these two polymers, so a large difference in the thickness dependence on the modulus might not be expected. However, the modulus of PnPMA, having a lower quench depth ($T_{g,bulk} = 36.1$ °C), begins to deviate from the bulk value at a significantly larger length scale of $\approx$80 nm, decreasing to 0.38 GPa at $\approx$20 nm, or 31% of its bulk modulus. This correspondence between bulk quench into the glass ($T_{g,bulk} − T$) and film thickness where deviations in modulus occur is consistent with predictions from simulations.[42] However, it is not clear if this change in moduli is homogeneous through the film or is a surface/interface effect.

In an effort to quantify the free surface effects on the measured modulus, a simple two-layer model has been proposed consisting of a surface layer of fixed thickness with a modulus that deviates from the bulk and the remainder of the film that behaves bulk-like.[44] This model is likely an extreme simplification of a potential gradient in modulus that extends from the free surface, similar to proposed gradients in T_g.[15] However, without a clear idea of the shape of the gradient, the two-layer approach provides a model with a minimal number of fitting parameters. Details regarding the bilayer model are found elsewhere.[44] Briefly, the model consists of a polymer film of thickness h_f containing two distinct moduli. The near surface of the film has a modulus of $E*$, and this surface layer extends a finite distance, δ, into the film; this surface layer is invariant with film thickness. The remainder of the film ($h_f − \delta$) exhibits a bulk-like modulus (E_{bulk}). From wrinkling mechanics, the expression for the wavelength takes the form[44]

where

$$\xi = \frac{\overline{E_{bulk}}\left(1 - \frac{\delta}{h_f}\right) + \overline{E*}\left(\frac{\delta}{h_f}\right)\left(2 - \frac{\delta}{h_f}\right)}{\overline{E_{bulk}}\left(1 - \frac{\delta}{h_f}\right) + \overline{E*}\left(\frac{\delta}{h_f}\right)} \quad (3)$$

The dashed lines in Figure 5 correspond to the best fits of the data to this bilayer model for the thickness of the surface layer, δ, and surface ($E*$) and bulk (E_{bulk}) moduli. The resultant fitting parameters from this model are shown in Table 2. To a first approximation, δ and h_f* are similar measures of the free surface layer thickness. For small δ and h_f* ($<$10 nm), the two measures are nearly indistinguishable within the uncertainty of the fits. This equivalence has been shown previously for films of PS and PMMA where $\delta < 5$ nm.[35] However, as the surface layer thickness increases, h_f* tends to underestimate δ due to nonlinearity in the relationship between λ and δ (as shown in eq 2). From the bilayer model fit, the surface layer thickness and its modulus can both be estimated. In all cases, the surface modulus is at least an order of magnitude less than the bulk for the best fit, but the fit is relatively insensitive to further decreases in the surface modulus. Note that this simple model captures the change in apparent moduli of all three polymers as a function of film thickness. For very thick films, the surface effect is negligible. As the film thickness is reduced, the thickness of the soft, near surface layer becomes comparable to the total film thickness and thus results in an apparent decrease in the film modulus. Additionally, as the quench depth decreases, the thickness of the free surface layer increases, thus leading to an earlier onset of deviation in modulus as film thickness is reduced.
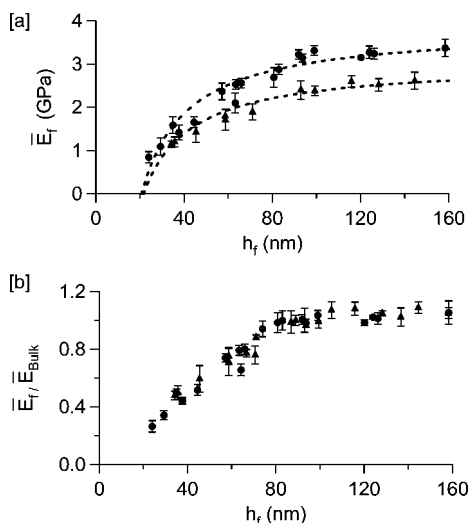
To further illustrate our hypothesis that the quench depth dictates the critical length scale for confinement-induced modulus changes, we investigated two methacrylate polymers with similar T_g but different bulk moduli: poly(isobutyl methacrylate) (PiBMA, $E_{bulk} = 1.98$ GPa, $T_{g,bulk} = 47$ °C) and poly(benzyl methacrylate) (PBzMA, $E_{bulk} = 2.69$ GPa, $T_{g,bulk} = 54$ °C). Figure 6a shows the apparent moduli of both polymers as a function of film thickness. The film thickness dependence exhibits similar features to the previous series: a plateau of their bulk moduli at large thicknesses followed by significant decrease in moduli as the film thickness is decreased. Comparison of the moduli of the two polymers in thin films appears to show a common length scale ($\approx$70 nm) where a deviation from the bulk-like moduli occurs. This is consistent with a correlation between the deviation length scale and quench depth into the glass for thin polymer films,[24] as the modulus

$$\lambda = 2\pi h_f\left(\frac{\overline{E_{bulk}}\left(1 - \frac{\delta}{h_f}\right)^3 + \overline{E*}\left(\frac{\delta}{h_f}\right)^3 + 3\overline{E_{bulk}}\left(1 - \frac{\delta}{h_f}\right)\left(1 - \xi - \frac{\delta}{h_f}\right)^2 + 3\overline{E*}\left(\frac{\delta}{h_f}\right)\left(2 - \xi - \frac{\delta}{h_f}\right)^2}{3E_s}\right)^{1/3} \quad (2)$$

TABLE 2. Fit Parameters for the Bilayer Model To Describe the Film Thickness Dependence of the Modulus (E^* Corresponds to the Modulus of the Surface Layer Having a Thickness δ)
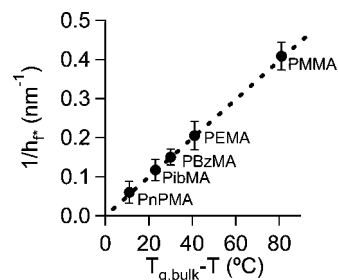
	PMMA	PEMA	PnPMA	PiBMA	PBzMA
E_{bulk} (GPa)	3.50 ± 0.12	1.70 ± 0.04	1.06 ± 0.05	2.23 ± 0.08	2.81 ± 0.05
E^* (GPa)	0.26 ± 0.25	0.08 ± 0.03	0.039 ± 0.02	0.042 ± 0.02	0.05 ± 0.02
δ (nm)	3.5 ± 0.1	9.8 ± 1.3	22.2 ± 2.7	21.6 ± 1.5	20.7 ± 1.9

Figure 7. Correlation between free surface layer thickness (h_f^*) and quench depth into the glass for the five poly-methacrylates examined. The dashed line is a linear fit of the data, and the error bars represent one standard deviation of the data, which is taken as the experimental uncertainty of the measurement.

of the bulk PiBMA is only approximately 70% of that of PBzMA. To better illustrate the similarity in the thin film behavior between PiBMA and PBzMA, Figure 6b shows the reduced modulus ($\bar{E}_f/\bar{E}_{bulk}$). The collapse of the data is similar to that reported previously for PS and PMMA films, which also have similar bulk T_g's.[35] Additionally, the moduli of these films can be fit with the bilayer model with an order of magnitude decrease in the modulus at the near surface of the films.

Although these data qualitatively illustrate that as bulk T_g is approached there is an increase in the size scale where deviations in modulus occur, a more quantitative description of the dependence of thin film modulus on quench depth into the glass ($T_{g,bulk} - T$) is desired. From the data, the near surface layer as defined by h_f^* appears to be an important factor in the thin film modulus behavior. Figure 7 illustrates how h_f^* scales with quench depth. Note that each data point represents a different poly(methacrylate). Simulations have noted that near T_g the thickness of the free surface layer can nearly extend throughout a thin film.[42] Using h_f^* as an experimental measure for this soft surface layer, it can be seen that extrapolation of the data from the five polymers examined here to $T = T_g$ results in $h_f^* \approx \infty$. Thus near T_g, the soft surface layer would be expected to extend throughout the thickness of a

thin polymer film as predicted by simulation.[42] The apparent inverse relationship of the soft layer thickness with quench depth could provide a facile route to estimating the elastic modulus of polymer nanostructures if this trend is universal for polymers. For example, this relationship could provide a facile route to predicting the impact of nanostructuring on the stability of the features by simply knowing the quench depth into the bulk glass at the processing conditions of interest by assuming that the near surface h_f^* does not support any stress (liquid-like). However, additional experimental and theoretical work is necessary to further elucidate the origins of this relationship and the applicability to other polymer systems. One hypothesis is that this temperature dependence of the soft surface layer is related to growth of the surface region of enhanced mobility of the polymer segments, similar to the growth of the liquid phase from the free interface into glassy tris-naphthylbenzene.[62] The results suggest that the modulus deviations observed in thin glassy polymer films are significantly influenced by the quench depth into the glass ($T_{g,bulk} - T$). Additionally, there exists a clear need to determine the local distribution of moduli in these films in order to gain further insight into nature of the surface effect.

CONCLUSIONS

In summary, the thin film moduli for a series of poly(methacrylates) were determined using wrinkling on an elastic substrate. As film thickness decreased below a critical threshold, the moduli also decreased in comparison to bulk values for all five polymers examined. However, the length scale at which deviations in moduli occurred depends upon the polymer and its bulk T_g. As the quench depth into the bulk glass decreases, the critical thickness at which the polymer film exhibits deviations from bulk-like values progressively increases to larger thicknesses, in agreement with discontinuous molecular dynamics simulations. Additionally, changes in the modulus of PnPMA thin films do not directly correlate with the thin film T_g behavior of identical films; this result raises questions to the applicability of fundamental polymer concepts, such the WLF equation, that

Figure 6. (a) Moduli of PiBMA (▲) and PBzMA (●). (b) Normalized moduli of PiBMA (▲) and PBzMA (●). The data show differing bulk moduli for both films with similar deviations observed at ≈85 nm. The lines are a fit to the bilayer model, and the error bars represent one standard deviation of the data, which is taken as experimental uncertainty of the measurement.

relate T_g to other physical properties. These results have direct implications in assessing the robustness of polymeric nanostructures critical for future microelectronics.

METHODS

Poly(methyl methacrylate) (PMMA) was purchased from Polymer Source (M_w = 91 kg/mol, T_g = 105 °C). Four other methacrylate polymers, poly(ethyl methacrylate) (PEMA) (M_w = 250 kg/mol, T_g = 65 °C), poly(n-propyl methacrylate) (PnPMA) (M_w = 70 kg/mol, T_g = 36.1 °C), poly(benzyl methacrylate) (PBzMA) (M_w = 70 kg/mol, T_g = 54 °C), and poly(isobutyl methacrylate) (PibMA) (M_w = 200 kg/mol, T_g = 47 °C), were obtained from Scientific Polymer Products. M_w is the mass average relative molecular mass. The T_g of each methacrylate polymer was determined from the discontinuity in the CTE of thick (>100 nm) films using ellipsometry as reported previously.[30] Note that certain commercial equipment, instruments, or materials are identified in this document. Such identification does not imply recommendation or endorsement by the National Institute of Standards and Technology (NIST) nor does it imply that the products identified are necessarily the best available for this purpose.

Polymer films of uniform thickness were spin-cast from dilute solutions in toluene onto mica substrates. PDMS (Sylgard 184, Dow Corning) was prepared at a ratio of 20:1 by mass of base to curing agent and allowed to gel at room temperature for 3 h before curing at 100 °C for 2 h. The thickness of the PDMS sheet was 1.5 mm. After cooling, the PDMS was cut into 2.5 cm × 7.5 cm strips. The modulus of the PDMS was determined using an Instron at a strain rate of 0.01 mm/s and found to be 0.7 ± 0.2 MPa. In order to exceed the critical strain required to produce surface wrinkling on all samples, the PDMS was prestrained to 4% using a stage described previously.[48] The polymer film was then transferred to strained PDMS using differential adhesion in water. The sample was dried under vacuum at 10 °C below its bulk T_g to avoid thermal-induced wrinkling. The prestrain on the PDMS was released at a rate of 0.1 mm/s. All samples were released at ambient temperature (T = 22 ± 2 °C). The thickness of the polymer film on the strained PDMS was determined using a variable angle spectroscopic ellipsometer (VASE M-2000, J.A. Woollam Co., Inc.) over a wavelength range from 250 to 1700 nm using three incident angles, 67, 70, and 73°. The data were modeled using the optical properties of the PDMS substrate and a Cauchy layer to describe the polymer film. The film thickness measured before transfer was found to be within 1 nm of the film thickness after transfer.

Characterization of the wrinkled surfaces was performed using atomic force microscopy (AFM) and optical microscopy. AFM images were acquired at ambient temperature on an Agilent Technologies 5500 system in tapping mode using a constant scan size of 7.5 μm × 7.5 μm at a scan rate of 1 Hz. AFM images were analyzed using 1D fast Fourier transform to obtain the wavelength of the wrinkles. Optical images were acquired using a Mititoyo Ultraplan FS-110 and analyzed using 1D fast Fourier transform in Matlab.

To measure the T_g of PnPMA thin films on PDMS, 20:1 PDMS films were spin-cast onto clean silicon wafers from a dilute toluene solution (0.5% by mass PDMS) and cured at 100 °C for 2 h. The PDMS layer was approximately 12 nm thick. The polymer film was transferred to the PDMS film from mica as described above. Ellipsometry was used to measure the thermal response of PDMS films and PDMS/PnPMA bilayers. T_g was determined from changes in the PnPMA film thickness measured upon cooling from 60 to 30 °C at 1.0 °C/min in a nitrogen purge atmosphere. To avoid aging artifacts, the measurements were performed by cooling from the rubbery state into the glass.

Supporting Information Available: Detailed description of wrinkling mechanics and a brief explanation of why the change in mechanical properties with film thickness is attributed to the thin polymer films and not the PDMS substrate are included as Supporting Information. Additionally, a representative micrograph of a smooth PDMS substrate prior to polymer film transfer is provided. This material is available free of charge *via* the Internet at http://pubs.acs.org.

REFERENCES AND NOTES

1. Williams, M. L.; Landel, R. F.; Ferry, J. D. Mechanical Properties of Substances of High Molecular Weight 0.19. The Temperature Dependence Of Relaxation Mechanisms in Amorphous Polymers and Other Glass-Forming Liquids. *J. Am. Chem. Soc.* **1955**, *77*, 3701–3707.
2. Ferry, J. D. *Viscoelastic Properties of Polymers*, 3rd ed.; John Wiley and Sons: New York, 1980.
3. Ngai, K. L.; Plazek, D. J. Identification of Different Modes of Molecular Motion in Polymers That Causes Thermorheological Complexity. *Rubber Chem. Technol.* **1995**, *68*, 376–384.
4. Mackay, M. E.; Dao, T. T.; Tuteja, A.; Ho, D. L.; Van Horn, B.; Kim, H.; Hawker, C. J. Nanoscale Effects Leading to Non-Einstein-like Decrease in Viscosity. *Nat. Mater.* **2003**, *22*, 762–766.
5. Cappella, B.; Kaliappan, S. K.; Sturm, H. Using AFM Force-Distance Curves to Study the Glass-to-Rubber Transition of Amorphous Polymers and Their Elastic−Plastic Properties as a Function of Temperature. *Macromolecules* **2005**, *38*, 1874–1881.
6. Ozin, G. A.; Yang, S. M. The Race for the Photonic Chip: Colloidal Crystal Assembly in Silicon Wafers. *Adv. Funct. Mater.* **2001**, *11*, 95–104.
7. Hartschuh, R.; Ding, Y.; Roh, J. H.; Kisliuk, A.; Sokolov, A. P.; Soles, C. L.; Jones, R. L.; Hu, T. J.; Wu, W. L.; Mahorowala, A. P. Brillouin Scattering Studies of Polymeric Nanostructures. *J. Polym. Sci., Part B: Polym. Phys.* **2004**, *42*, 1106–1113.
8. Lei, J.; Fan, J.; Yu, C. Z.; Zhang, L. Y.; Jiang, S. Y.; Tu, B.; Zhao, D. Y. Immobilization of Enzymes in Mesoporous Materials: Controlling the Entrance to Nanospace. *Microporous Mesoporous Mater.* **2004**, *73*, 121–128.
9. Solak, H. H.; David, C.; Gobrecht, J.; Golovkina, V.; Cerrina, F.; Kim, S. O.; Nealey, P. F. Sub-50 nm Period Patterns with EUV Interference Lithography. *Microelectron. Eng.* **2003**, *67*, 56–62.
10. Chou, S. Y.; Krauss, P. R.; Renstrom, P. J. Imprint Lithography with 25-Nanometer Resolution. *Science* **1996**, *272*, 85–87.
11. Rowland, H. D.; King, W. P.; Pethica, J. B.; Cross, G. L. W. Molecular Confinement Accelerates Deformation of Entangled Polymers during Squeeze Flow. *Science* **2008**, *322*, 720–722.
12. Ding, Y.; Ro, H.; Douglas, J. F.; Jones, R. L.; Karim, A.; Soles, C. L. Polymer Viscoelasticity and Residual Stress Effects on Nanoimprint Lithography. *Adv. Mater.* **2007**, *19*, 1377–1382.
13. Bansal, A.; Yang, H. C.; Li, C. Z.; Cho, K. W.; Benicewicz, B. C.; Kumar, S. K.; Schadler, L. S. Quantitative Equivalence between Polymer Nanocomposites and Thin Polymer Films. *Nat. Mater.* **2005**, *4*, 693–698.
14. Rittigstein, P.; Priestley, R. D.; Broadbelt, L. J.; Torkelson, J. M. Model Polymer Nanocomposites Provide an Understanding of Confinement Effects in Real Nanocomposites. *Nat. Mater.* **2007**, *6*, 278–282.
15. Ellison, C. J.; Torkelson, J. M. The Distribution of Glass-Transition Temperatures in Nanoscopically Confined Glass Formers. *Nat. Mater.* **2003**, *2*, 695–700.

16. Forrest, J. A.; Mattsson, J. Reductions of the Glass Transition Temperature in Thin Polymer Films: Probing the Length Scale of Cooperative Dynamics. *Phys. Rev. E* **2000**, *61*, 153–156.

17. Keddie, J. L.; Jones, R. A. L. Size-Dependent Depression of the Glass Transition Temperature in Polymer Films. *Europhys. Lett.* **1994**, *27*, 59–64.

18. Kim, J. H.; Jang, J.; Zin, W. C. Estimation of the Thickness Dependence of the Glass Transition Temperature in Various Thin Polymer Films. *Langmuir* **2000**, *16*, 4064.

19. Torres, J. A.; Nealey, P. F.; de Pablo, J. J. Molecular Simulation of Ultrathin Polymeric Films near the Glass Transition. *Phys. Rev. Lett.* **2000**, *85*, 3221–3224.

20. Alcoutlabi, M.; McKenna, G. B. Effects of Confinement on Material Behaviour at the Nanometre Size Scale. *J. Phys.: Condens. Matter* **2005**, *17*, R461–R524.

21. Lin, E; Kolb, R.; Satija, S.; Wu, W. Reduced Polymer Mobility Near the Polymer/Solid Interface as Measured by Neutron Reflectivity. *Macromolecules* **1999**, *32*, 3753–3754.

22. Ellison, C. J.; Munda, M. K.; Torkelson, J. M. Impacts of Polystyrene Molecular Weight and Modification to the Repeat Unit Structure on the Glass Transition-Nanoconfinement Effect and the Cooperativity Length Scale. *Macromolecules* **2005**, *38*, 1767–1778.

23. Singh, L.; Ludovice, P. J.; Henderson, C. L. Influence of Molecular Weight and Film Thickness on the Glass Transition Temperature and Coefficient of Thermal Expansion of Supported Ultrathin Polymer Films. *Thin Solid Films* **2003**, *449*, 231–241.

24. Bohme, T. R.; de Pablo, J. J. Evidence for Size-Dependent Mechanical Properties from Simulations of Nanoscopic Polymeric Structures. *J. Chem. Phys.* **2002**, *116*, 9939–9951.

25. Tsui, T. Y.; Pharr, G. M. Substrate Effects on Nanoindentation Mechanical Property Measurement of Soft Films on Hard Substrates. *Mater. Res.* **1999**, *14*, 292–301.

26. Shulha, H.; Kovalev, A.; Myshkin, N.; Tsukruk, V. V. Some Aspects of AFM Nanomechanical Probing of Surface Polymer Films. *Eur. Polym. J.* **2004**, *40*, 949–956.

27. Tweedie, C. A.; Constantinides, G.; Lehman, K. E.; Brill, D. J.; Blackman, G. S.; Van Vliet, K. J. Enhanced Stiffness of Amorphous Polymer Surfaces under Confinement of Localized Contact Loads. *Adv. Mater.* **2007**, *19*, 2540–2547.

28. Maranganti, R.; Sharma, P. A Novel Atomistic Approach to Determine Strain-Gradient Elasticity Constants: Tabulation and Comparison for Various Metals, Semiconductors, Silica, Polymers and the (Ir) Relevance for Nanotechnologies. *J. Mech. Phys. Solids* **2007**, *55*, 1823–1852.

29. Miyake, K.; Satomi, N.; Sasaki, S. Elastic Modulus of Polystyrene Film from Near Surface to Bulk Measured by Nanoindentation Using Atomic Force Microscopy. *Appl. Phys. Lett.* **2006**, *89*, 319251–319253.

30. Meyers, G. F.; Dekoven, B. M.; Seitz, J. T. Is the Molecular-Surface of Polystyrene Really Glassy? *Langmuir* **1992**, *8*, 2330–2335.

31. Forrest, J. A.; DalnokiVeress, K.; Stevens, J. R.; Dutcher, J. R. Effect of Free Surfaces on the Glass Transition Temperature of Thin Polymer Films. *Phys. Rev. Lett.* **1996**, *77*, 2002–2005.

32. Forrest, J. A.; Dalnoki-Veress, K.; Dutcher, J. R. Brillouin Light Scattering Studies of the Mechanical Properties of Thin Freely Standing Polystyrene Films. *Phys. Rev. E* **1998**, *58*, 6109–6114.

33. Hartschuh, R. D.; Kisliuk, A.; Novikov, V.; Sokolov, A. P.; Heyliger, P. R.; Flannery, C. M.; Johnson, W. L.; Soles, C. L.; Wu, W. L. Acoustic Modes and Elastic Properties of Polymeric Nanostructures. *Appl. Phys. Lett.* **2005**, *87*, 173121.

34. Stoykovich, M. P.; Yoshimoto, K.; Nealey, P. F. Mechanical Properties of Polymer Nanostructures: Measurements Based on Deformation in Response to Capillary Forces. *Appl. Phys. A* **2008**, *90*, 277–283.

35. Stafford, C. M.; Vogt, B. D.; Harrison, C.; Julthongpiput, D.; Huang, R. Elastic Moduli of Ultrathin Amorphous Polymer Films. *Macromolecules* **2006**, *39*, 5095–5099.

36. Grohens, Y.; Hamon, L.; Reiter, G.; Soldera, A.; Holl, Y. Some Relevant Parameters Affecting the Glass Transition of Supported Ultra-thin Polymer Films. *Eur. Phys. J. E* **2002**, *8*, 217–224.

37. Forrest, J. A.; Danoki-Veress, K. The Glass Transition in Thin Polymer Films. *Adv. Colloid Interface Sci.* **2001**, *94*, 167–196.

38. Tsui, O. K. C.; Russell, T. P.; Hawker, C. J. Effect of Interfacial Interactions on the Glass Transition of Polymer Thin Films. *Macromolecules* **2001**, *34*, 5535–5539.

39. Campbell, C. G.; Vogt, B. D. Examination of the Influence of Cooperative Segmental Dynamics on the Glass Transition and Coefficient of Thermal Expansion in Thin Films Probed Using Poly(*n*-alkyl methacrylate)s. *Polymer* **2007**, *48*, 7169–7175.

40. Forrest, J. A.; Dalnoki-Veress, K.; Dutcher, J. R. Brillouin Light Scattering Studies of the Mechanical Properties of Thin Freely Standing Polystyrene Films. *Phys. Rev. E* **1998**, *58*, 6109–6114.

41. Rogers, S. S.; Madlkern, L. Glass Transitions of the Poly(*n*-alkyl methacrylates). *J. Phys. Chem.* **1957**, *61*, 985–991.

42. Yoshimoto, K.; jain, T.; Nealey, P. F.; de Pablo, J. J. Local Dynamic Mechanical Properties in Model Free-Standing Polymer Thin Films. *J. Chem. Phys.* **2005**, *122*, 144712.

43. Stafford, C. M.; Harrison, C.; Beers, K. L.; Karim, A.; Amis, E. J.; Vanlandingham, M. R.; Kim, H. C.; Volksen, W.; Miller, R. D.; Simonyi, E. E. A Buckling-Based Metrology for Measuring the Elastic Moduli of Polymeric Thin Films. *Nat. Mater.* **2004**, *3*, 545–550.

44. Huang, R.; Stafford, C. M.; Vogt, B. D. Effect of Surface Properties on Wrinkling of Ultrathin Films. *J. Aero. Eng.* **2007**, *20*, 38–44.

45. Wilder, E. A.; Gup, S.; Lin-Gibson, S.; Fasolka, M. J.; Stafford, C. M. Measuring the Modulus of Soft Polymer Networks *via* a Buckling-Based Metrology. *Macromolecules* **2006**, *39*, 4138–4143.

46. Mei, H. X.; Huang, R.; Chung, J. Y.; Stafford, C. M.; Yu, H. H. Buckling Modes of Elastic Thin Films on Elastic Substrates. *Appl. Phys. Lett.* **2007**, *90*, 1519021–1519023.

47. Harrison, C.; Stafford, C. M.; Zhang, W. H.; Karim, A. Sinusoidal Phase Grating Created by a Tunably Buckled Surface. *Appl. Phys. Lett.* **2004**, *85*, 4016–4018.

48. Stafford, C. M.; Guo, S.; Harrison, C.; Chiang, M. Y. M. Combinatorial and High-Throughput Measurements of the Modulus of Thin Polymer Films. *Rev. Sci. Instrum.* **2005**, *76*, 062207.

49. Van Zanten, J. H.; Wallace, W. E.; Wu, W. Effect of Strongly Favorable Substrate Interactions on the Thermal Properties of Ultrathin Polymer Films. *Phys. Rev. E* **1996**, *53*, R2053–R2056.

50. Wallace, W. E.; Van Zanten, J. H.; Wu, W. Influence of an Impenetrable Interface on a Polymer Glass-Transition Temperature. *Phys. Rev. E* **1995**, *52*, R3329–R3332.

51. Hartschuh, R.; Ding, Y.; Roh, J. H.; Kisliuk, A.; Sokolov, A. P.; Soles, C. L.; Jones, R. L.; Hu, T. J.; Wu, W. L.; Mahorowala, A. P. Brillouin Scattering Studies of Polymeric Nanostructures. *J. Polym. Sci., Part B: Polym. Phys.* **2004**, *42*, 1106–1114.

52. Sun, L.; Dutcher, J. R.; Giovanni, L.; Nizzoli, F.; Stevens, J. R.; Ord, J. L. Elastic and Elasto-Optic Properties of Thin Films of Poly(styrene) Spin Coated onto Si(001). *J. Appl. Phys.* **1994**, *75*, 7482–7488.

53. O'Connell, P. A.; McKenna, G. B. Rheological Measurements of the Thermoviscoelastic Response of Ultrathin Polymer Films. *Science* **2005**, *307*, 1760–1763.

54. Priestley, R. D.; Ellison, C. J.; Broadbelt, L. J.; Torkelson, J. M. Structural Relaxation of Polymer Glasses at Surfaces, Interfaces, and In Between. *Science* **2005**, *309*, 456–459.

55. Tseng, K. C.; Turro, N. J.; Durning, C. J. Molecular Mobility in Polymer Thin Films. *Phys. Rev. E* **2000**, *61*, 1800–1811.

56. Mansfield, K. F.; Theodorou, D. N. Molecular-Dynamics Simulation of a Glassy Polymer Surface. *Macromolecules* **1991**, *24*, 6283–6294.

57. Jain, T. S.; de Pablo, J. J. Investigation of Transition States in Bulk and Freestanding Film Polymer Glasses. *Phys. Rev. Lett.* **2004**, *92*, 155505–155508.

58. Jain, T. S.; de Pablo, J. J. Influence of Confinement on the Vibrational Density of States and the Boson Peak in a Polymer Glass. *J. Chem. Phys.* **2004**, *120*, 9371–9375.

59. Korkmaz, T.; Dogan, A.; Usanmaz, A. Dynamic Mechanical Analysis of Provisional Resin Materials Reinforced by Metal Oxides. *Biomed. Mater. Eng.* **2005**, *15*, 179–188.

60. Seitz, J. T. The Estimation of Mechanical Properties of Polymers from Molecular Structure. *J. Appl. Polym. Sci.* **1993**, *49*, 1331–1351.

61. Van Spegen, W. M.; Tambe, N. S.; Sullivan, B.; Tyndal, G. W.; Sun, Y.; Vettiger, P.; Swanson, P.; Wei, G.; Wendell, D.; Zorman, C. A.; Young, D. J.; Zoval, J.; Shu, Y. E.; Ziaie, B.; Zysset, P. K. Mechanical Properties of Nanostructures In *Nano-Technology*, 2nd ed.; Bushan, B., Ed.; Springer: Berlin, 2007; pp 1305−1334.

62. Swallen, S. F.; Traynor, K.; McMahon, R. J.; Ediger, M. D.; Mates, T. E. Stable Glass Transformation to Supercooled Liquid *via* Surface-Initiated Growth Front. *Phys. Rev. Lett.* **2009**, *102*, 655031–655034.